

Wavelength and Bandwidth Allocation for Mobile Fronthaul in TWDM-PON

Yu Nakayama^{id}, *Member, IEEE*, and Daisuke Hisano^{id}, *Member, IEEE*

Abstract—Time- and wavelength- division multiplexed passive optical network (TWDM-PON) has attracted considerable attention for the next generation optical access systems. Among potential applications of TWDM-PON, a major application is the support of mobile fronthaul streams between radio units (RUs) and distributed units (DUs) in the centralized radio access network (C-RAN) architecture, which consists of central units (CUs), DUs, and RUs. The upstream fronthaul traffic that an optical line terminal (OLT) receives is expected to become highly bursty due to the variable data rate generated by employing new functional split options and the synchronization of data transmission between neighboring RUs caused by time-division duplex (TDD). However, there has been no wavelength and bandwidth allocation scheme for TWDM-PON that is designed to efficiently accommodate fronthaul streams satisfying the strict delay requirement. Therefore, in this paper we propose a novel wavelength and bandwidth allocation algorithm that can minimize the number of active wavelength channels considering the high burstiness and delay requirement of fronthaul data transmission. Through computer simulations it was confirmed that the number of active wavelength channels can be reduced by 50% with the proposed algorithm, and thus more RUs can be efficiently accommodated using TWDM-PON.

Index Terms—Bandwidth, Optical network units, Base stations, Wireless communication, Channel allocation, Uplink.

I. INTRODUCTION

CENTRALIZED radio access network (C-RAN) architecture has been extensively developed to efficiently forward the ever increasing traffic of mobile devices [1]. With the C-RAN architecture, a large number of small cells are densely deployed to enhance the network capacity [2]. This is enabled by splitting the functions of a mobile base station (BS) into three components as shown in Fig. 1; a central unit (CU), a distributed unit (DU), and a radio unit (RU) [3]. The link between a DU and an RU is called fronthaul, and the link between a CU and a DU is called midhaul. The fronthaul transmission has strict latency requirements, e.g. $\leq 100 \mu\text{s}$ [4] and $\leq 250 \mu\text{s}$ [5]. To reduce the amount of data transmitted via the common public radio interface (CPRI), which has been the

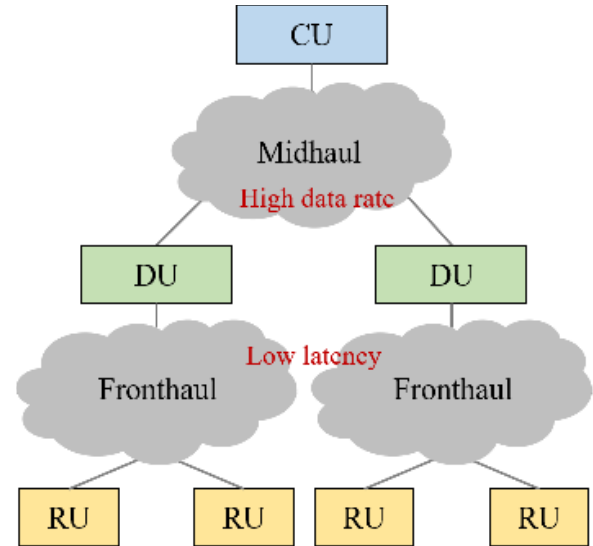


Fig. 1. C-RAN architecture.

typical and widespread fronthaul interface, new functional split options are under consideration [4], [5]. With these options, the data rate becomes variable and proportional to the wireless link data rate. Furthermore, additional features for mobile networks that have effects on the fronthaul data transmission have been discussed for 5G networks, i.e. time-division duplex (TDD) and coordinated multipoint (CoMP) [6].

Passive optical network (PON) based mobile fronthaul has been proposed to improve the utilization of optical links and to deploy inexpensive fronthaul [7], [8]. PON has been one of the key technologies for providing low-cost access services. It is widely employed in today's fiber-to-the-home (FTTH) networks. The general architecture of PON is shown in Fig. 2. An optical line terminal (OLT) and optical network units (ONUs) are connected via the optical distribution network (ODN). The ODN is composed of optical fibers and passive power splitters installed in outside plants. Fig. 3 depicts the architecture of PON based mobile fronthaul. An OLT is located in a central office and connected with a DU. ONUs are located on antenna sites and linked with RUs. PON based fronthaul is expected to efficiently support spatio-temporally traffic fluctuation in small cells [9] by sharing optical fibers with multiple cells [7].

Currently, 10 Gigabit class time division multiplexed (TDM)-PON systems, such as 10Gigabit-Ethernet PON (10G-EPON) [10] and 10-Gigabit-capable PON (XG-PON) [11] are generally deployed. The next step for optical access systems

Manuscript received January 16, 2019; revised May 5, 2019 and June 30, 2019; accepted August 28, 2019. Date of publication September 3, 2019; date of current version November 19, 2019. This work was supported by JST, ACT-I, Grant Number JPMJPR18UL, Japan. The associate editor coordinating the review of this article and approving it for publication was A. Chaaban. (*Corresponding author: Yu Nakayama.*)

Y. Nakayama is with the Institute of Engineering, Tokyo University of Agriculture and Technology, Tokyo 184-8588, Japan (e-mail: yu.nakayama@ieec.org).

D. Hisano is with the Graduate School of Engineering, Osaka University, Osaka 565-0871, Japan

Color versions of one or more of the figures in this article are available online at <http://ieeexplore.ieee.org>.

Digital Object Identifier 10.1109/TCOMM.2019.2939319

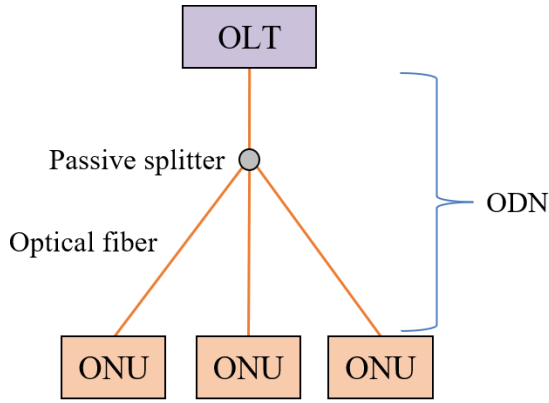


Fig. 2. General architecture of PON.

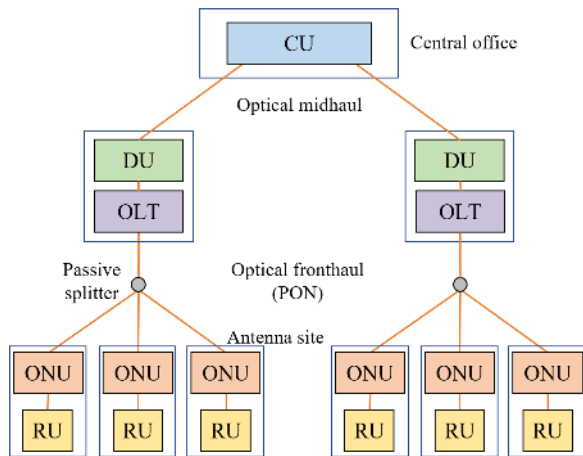


Fig. 3. Architecture of PON based fronthaul.

is time- and wavelength- division multiplexed (TWDM)-PON systems such as next generation-PON2 (NG-PON2) [12]. NG-PON2 is a 40 Gb/s capacity PON system that exploits the time and wavelength (λ) domains [13], [14]. TWDM-PON is expected to be a multi-service platform that provides mobile, business, residential, machine to machine (M2M), and Internet of things (IoT) services.

An important research topic for PON based fronthaul has been optimally allocating upstream bandwidth to satisfy large bandwidth and strict low-latency requirements of mobile fronthaul traffic [15]. There have been many research efforts for efficiently accommodating fronthaul traffic in TDM-PON, e.g. a mobile dynamic bandwidth allocation (DBA) proposed in [16]. In the 5G and beyond 5G era, the upstream bandwidth allocation problem becomes more severe, because the upstream traffic in the upstream link in PON becomes highly bursty due to the variable data rate and the synchronization of data transmission between neighboring RUs with the TDD systems. That is, it will be difficult to accommodate a large number of ONUs using small number of wavelength channels because of the bandwidth limitation. Although many wavelength and bandwidth allocation algorithms have been proposed for TWDM-PON, these algorithms cannot be employed for fronthaul transmission because the average delay usually exceeds several milliseconds, i.e. the strict latency requirements cannot be satisfied. Also, the previous studies

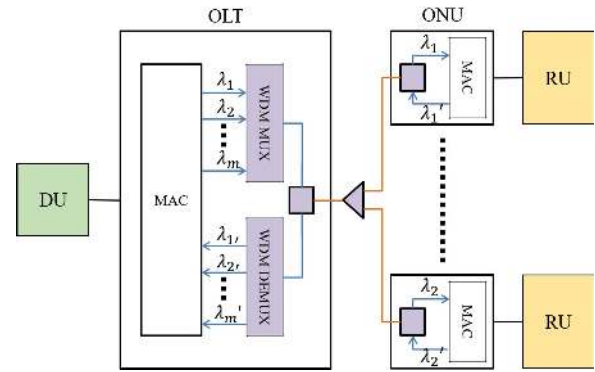


Fig. 4. TWDM system diagram.

on TWDM-PON based fronthaul have not fully investigated the latency problem under the characteristic upstream traffic in the TDD system.

To address this problem, this paper proposes a novel wavelength and bandwidth allocation algorithm for TWDM-PON with mobile fronthaul traffic. The contribution of the paper is to propose an algorithm that can achieve efficient accommodation of TDD-based fronthaul satisfying the strict latency requirements. The basic idea of the proposed algorithm is based on the characteristics of TDD fronthaul traffic: (1) the maximum burst size is determined by wireless parameters; (2) uplink/downlink data transmissions occur based on time-synchronization between neighboring RUs. The purpose of the proposed algorithm is to minimize the number of active wavelength channels, which is equivalent to maximize the number of assigned ONUs per channel. Thus, minimizing the active wavelengths leads to the reduction in deployment cost and energy consumption of TWDM-PON based fronthaul. Although the basic idea was introduced in [17], it did not consider the synchronization timing error of TDD and the burst size generated with the 5G parameters. That is, although time-synchronization is performed among neighboring RUs in the TDD systems, certain values of timing error are assumed based on the defined categories [18]. The timing error can result in data transmission error or collision in the PON system. The formulation and algorithm is revised from the basic idea introduced in [17]. Also, we provide the detailed explanation with the mathematical proof on the proposed algorithm which is a polynomial time one and the computational complexity is $\mathcal{O}(M)$. In addition, we provide novel simulation results considering the synchronization timing error assuming the 5G parameters.

The rest of the paper is organized as follows. Section II summarizes related work and the contribution of this paper. The proposed algorithm is introduced in section III. Section IV describes the performance evaluation of the proposed algorithm with simulation results. The conclusion of this paper is provided in section V.

II. RELATED WORK

A. TWDM-PON

Fig. 4 depicts the general system diagram for TWDM-PON. This system architecture comprises a stack of multiple

TDM-PONs using m pairs of wavelength channels. The wavelength pairs are represented as $\{\lambda_1, \lambda_{1'}\}, \{\lambda_2, \lambda_{2'}\}, \dots, \{\lambda_m, \lambda_{m'}\}$. ONUs are equipped with tunable transmitters and receivers. The used wavelength of the transmitter and the receiver can be tuned to any of the upstream and downstream wavelengths, respectively. The management of the wavelength domain performed by the OLT is a key challenge with TWDM-PON.

For TWDM-PON, an automatic load-balancing wavelength and bandwidth allocation algorithm was proposed in [19], which is applicable despite the use of long-time tuning devices. The first-fit algorithm proposed in [20] can achieve low-latency by giving a grant to an ONU on a single channel which is available earliest among all the channels. The algorithms proposed in [21] achieve low-latency in long reach PON by employing the multi-threaded polling. An online gated algorithm was proposed in [22] to assign a flexible number of wavelengths and a dynamic grant size on each upstream wavelength. In [23], several online algorithms were investigated to utilize wavelength resources especially in the case of large differential distances of ONUs from the OLT. However, the average delay exceeds several hundred microseconds or several milliseconds with these algorithms; the maximum delay cannot be reduced to satisfy the strict latency requirements of fronthaul. This is because these algorithms are online algorithms based on the exchange of REPORT and GATE messages, and thus the increase in queuing delay is inevitable.

As regards energy savings, an energy-efficient framework for a delay-constrained TWDM-PON system was proposed in [24], [25]. The proposed framework optimizes the number of active wavelengths at the OLT and the sleep or doze time of the ONUs to reduce the energy consumption. When average bandwidth requested by an ONU exceeds the maximum bandwidth allowable for an ONU, the number of active wavelengths is incremented to satisfy delay constraints. If the bandwidth request becomes small, idle wavelengths are switched off to increase energy savings. A power-consumption model and a wavelength and bandwidth allocation algorithm was proposed in [26] to enhance the energy efficiency to address the penalties in terms of delay and power consumption when an ONU activates its transmissions on new wavelengths.

Another problem for dynamic wavelength allocation (DWA) is that the ONU channel handover sequence is usually accompanied with service disruptions. The wavelength optimization has to consider such service disruptions along with other aspects. In [27], the tradeoffs between load balancing, reconfiguration, and energy savings are investigated. To minimize the traffic migration and energy consumption as two objectives, a multi-objective integer linear program (MOILP) model was proposed.

B. Fronthaul With PON

The concept of PON-based mobile fronthaul has been a hot research topic for supporting the massive deployment of small cells [28]. There have been many research efforts for efficiently accommodating fronthaul traffic in TDM-PON. The conventional online and offline DBA algorithms such as IPACT [29] cannot be employed for fronthaul because it

takes too much time for exchanging the REPORT and GATE messages. An idea of the mobile DBA was proposed in [16] in order to guarantee the strict latency requirement of fronthaul in PON. The mobile DBA reduces the upstream queuing delay by utilizing the scheduling information of wireless domain. The authors of [30] proposed a DBA scheme for fronthaul based on simple statistical traffic analysis. With the proposed scheme, allocated bandwidth is gradually changed at the period of several-ten minutes or several hours. The experiments showed that excess bandwidth allocation is reduced from classic fixed bandwidth allocation (FBA) while achieving latency under $50 \mu\text{s}$. However, such statistical methods may drop packets if the data rate increases. A DBA method that automatically optimizes the cycle length to reduce the latency and improve bandwidth efficiency was proposed and demonstrated in [31], [32].

The concept of a virtual PON (VPON) with a virtual base station (VBS) was proposed in [33]. A VBS is dynamically formed for each cell by assigning virtualized network resources such as a virtualized fronthaul link and virtualized functional entities performing baseband processing in DU cloud. The VBS formation (VF) optimization problem was formulated and solved for energy savings using an integer linear program (ILP). This paper considered that the upstream latency always meets the requirements of fronthauling with a fixed bandwidth allocation proposed in [34], and did not investigate the latency problem at all. However, the authors of [34] only proposed the basic idea of using TWDM-PON for mobile fronthaul, and did not fully investigate the efficient allocation of wavelength and bandwidth. In [35], a distributed approach was proposed for formulating virtual TDM-PONs adaptively in a TWDM-PON-based C-RAN. They formulated game theoretic models considering a scenario where ONU have the initiative to choose a proper VPON to register to based on its knowledge on the C-RAN. The goal of this paper is to improve the scalability of VPON with distributed computing, and thus the latency problem was not fully investigated. As stated above, there has been no wavelength and bandwidth allocation scheme for TWDM-PON for efficiently accommodating a large number of mobile fronthaul streams. To address this problem, this paper proposes an allocation scheme considering the features of upstream traffic in the TDD system, which is explained in detail in II-C. Note that the proposal in this paper can coexist the concept of VPON.

C. TDD-Based Fronthaul

Here we explain the TDD-based fronthaul. The TDD system is expected to be widely employed in C-RAN. As an example, Fig. 5 shows the TDD configuration in LTE. In Fig. 5, “D” and “U” represent a sub-frame for downlink and uplink transmission, respectively. “S” represents a special sub-frame which is a guard period between downlink to uplink switching to reduce interference. The index 0–6 represents different uplink and downlink transmission combination. With the TDD system, the uplink and downlink data transmissions occur based on time-synchronization between neighboring RUs according to the used TDD configuration. For example, when the index 0 is employed among neighboring RUs, downlink

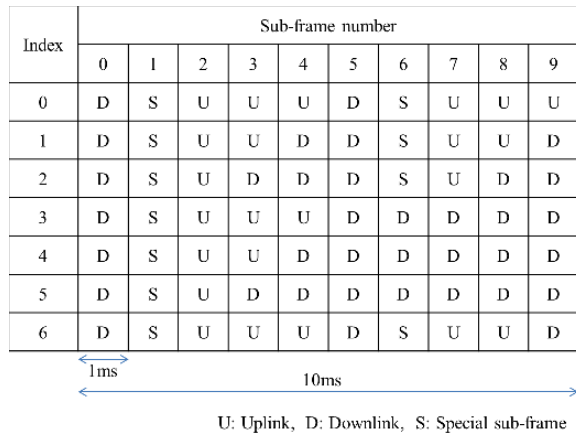


Fig. 5. TDD configuration in LTE.

transmission occurs in 0th sub-frame and uplink transmission occurs in 2nd sub-frame, and so on. This feature is unlike the frequency-division duplex (FDD) systems employed in LTE and LTE-Advanced, where RUs perform frequency-synchronization. With TDD, accurate time-synchronization is required to avoid collision between upstream and downstream data. The uplink/downlink transmission strictly follows the defined sub-frame in all neighboring RUs. Therefore, if multiple RUs are connected to a DU via a network, the upstream and downstream traffic becomes highly bursty. When PON is employed as shown in Fig. 3, if neighboring multiple RUs send upstream data at a sub-frame, ONUs receive uplink traffic at the same time, and thus the link between an OLT and ONUs is required to forward highly bursty upstream traffic. Note that the basic principle of TDD is independent of the configuration; the discussion here is applicable for any configuration including 5G and dynamic TDD. To reduce the delay in upstream links to satisfy the latency requirement of fronthaul has been an important research topic [36], [37].

When neighboring RUs are connected with PON as shown in Fig. 3, RUs time-synchronizedly send upstream data, and thus the ONUs synchronizedly receive upstream data. The ONUs simultaneously store the upstream data to send to the OLT in their transmission queues. That is, the traffic in the upstream link in PON becomes highly bursty with the TDD system. As a consequence, it is difficult to satisfy the strict delay requirement for fronthaul with small number of wavelength channels with existing algorithms. Therefore, considering the features of upstream traffic in the TDD system an optimized wavelength and bandwidth allocation scheme is required to efficiently accommodate TDD-based fronthaul streams with TWDM-PON.

There are four categories for the TDD time-synchronization requirements [18], which are shown in Table I. Synchronization accuracy is given using absolute time error values from reference points such as the International Atomic Time or the master clock in precision time protocol (PTP).

D. Tuning Time Class

A certain time is required for an ONU to finish the wavelength tuning process. In the case of NG-PON2, which is a

TABLE I
TDD TIME-SYNCHRONIZATION REQUIREMENTS

Category	Time error value
A+	< 12.5ns
A	< 45ns
B	< 110ns
C	< 1.5 μ s

TABLE II
WAVELENGTH CHANNEL TUNING TIME CLASS

Tuning time class	Tuning time
Class 1	< 10 μ s
Class 2	10 μ s – 25 ms
Class 3	25 ms – 1 s

typical TWDM-PON standard, tuning time classes are specified [38]. The tuning time classes are summarized in Table II. Each class of the ONU transmitter and receiver finishes the tuning process in the required tuning time. The class boundaries are broadly defined based on known tuning technologies.

The slowest (Class 3) is suited to applications where tuning operations are infrequent. Class 2 allows faster tuning to enable sub-50 ms protection. The fastest (Class 1) enables future dynamic wavelength and bandwidth allocation feature in the system [39].

E. Contribution

The contribution of this paper is summarized in the following. Although many wavelength and bandwidth allocation algorithms have been proposed for TWDM-PON, most of them were messaging-based, i.e. IPACT-based, algorithms. With these algorithms, the exchange of REPORT and GATE messages between an OLT and ONUs increases the queuing delay; the average delay usually exceeds several milliseconds. Since there are strict latency requirements for fronthaul such as $\leq 100 \mu$ s [4] and $\leq 250 \mu$ s [5], these algorithms cannot be employed for fronthaul transmission. The previous studies on TWDM-PON based fronthaul including VPON have not fully investigated the latency problem. In particular, there have never been algorithms for achieving efficient allocation of wavelength and bandwidth under the characteristic upstream traffic in the TDD system. The goal of this paper is to address this problem. Therefore, the contribution of the paper is to propose a wavelength and bandwidth allocation algorithm for TWDM-PON that can achieve efficient accommodation of TDD-based fronthaul streams satisfying the strict latency requirements.

In this paper we propose a novel wavelength and bandwidth allocation algorithm that minimizes active wavelength channels considering the globally synchronized fronthaul data transmission and different propagation delay for ONUs. The characteristics of TDD mobile fronthaul are that (1) maximum burst size of each stream is determined by wireless parameters and (2) timing synchronization between neighboring RUs. The first feature enables the estimation of the maximum burst size as the worst case for satisfying the latency requirements.

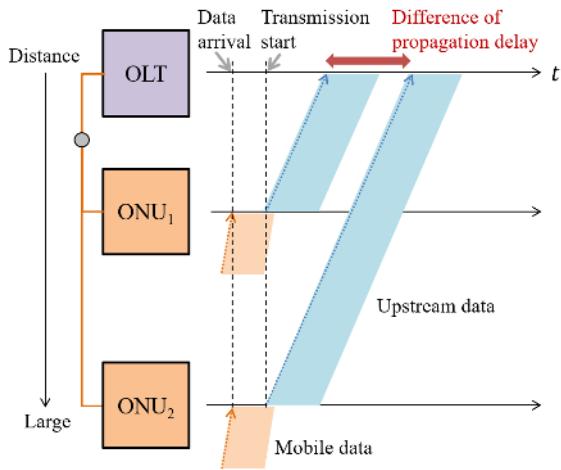


Fig. 6. Data transmission and reception time.

Because of the second feature, the upstream data reception timing at ONUs is predictable based on the estimation of the transmission time interval (TTI) cycle in the C-RAN. On the contrary, the worst case burst cannot be defined for usual traffic conditions, because the maximum burst size is not fixed and the arrival timing of each stream are not predictable. Thus, the contribution of the proposed algorithm is to efficiently accommodate fronthaul streams satisfying the latency requirements on the basis of the characteristics of TDD mobile fronthaul.

III. PROPOSED ALGORITHM

A. Concept

Here we introduce the concept of the proposed algorithm. The goal of the proposed algorithm is to minimize the number of active wavelength channels satisfying the strict latency requirements, which is equivalent to maximize the number of assigned ONUs per channel. This leads to the reduction in deployment cost and energy consumption of TWDM-PON based fronthaul. To this end, the proposed algorithm allocates wavelength and bandwidth based on the characteristics of TDD fronthaul traffic: (1) the maximum upstream burst data size is determined by wireless parameters; (2) uplink data transmissions occur based on time-synchronization between neighboring RUs.

Fig. 6 shows the relationship between data transmission and reception time of an OLT and ONUs in PON based fronthaul. In this diagram, two ONUs are allocated to the same PON wavelength channel and they receive the upstream mobile data from RUs. The data arrival timing is synchronized by the TDD system with a certain accuracy determined by the categories for synchronization requirements. Then, the ONUs send the upstream data. Even if they start to send the data at the same time, the arrival time at the OLT is different due to the difference in the propagation delay of optical signals. The data sent by 1st ONU arrives at the OLT faster because the distance to the OLT from this ONU is shorter than that from 2nd ONU. In case the propagation delay is the same for these two ONUs, an ONU waits for the data transmission of the other ONU

TABLE III
VARIABLES

Variable	Definition
i	ONU identifier
j	Time slot identifier ($j \geq 1$)
k	Wavelength channel identifier
M	Number of ONUs
N	Number of time slots
K	Number of wavelength channel
c	Allocation cycle identifier
T_{start}^c	Start time of c th cycle
T_j^c	Start of j th time slot of c th cycle
T_{lim}^c	Threshold for fronthaul data transmission of c th cycle
p_{min}	Minimum propagation delay
d_{onu}	Processing delay for an ONU
p_i	Propagation delay for i th ONU
q_i	Queuing delay for i th ONU
τ_i	Minimum time slot for i th ONU
B	Maximum burst size
L	Link speed of a PON channel
δ	Time period for data transmission
σ	Synchronization time error value

to avoid the signal collision in the optical fiber. This timing control is usually executed by the OLT with the upstream bandwidth allocation algorithm. The increase in the queuing delay at the ONU results in the increase in the worst case delay of the fronthaul streams. Consequently, the increase in the worst case delay reduces the expected number of allocatable ONUs for a wavelength channel.

To reduce the queuing delay, the proposed algorithm considers the relationship between data transmission and reception time, which is described above. The allowable delay and the constraint for allocation timing are formulated based on the different propagation delay between the OLT and ONUs. Then, the wavelength channel and upstream bandwidth are allocated to minimize the number of active wavelength channels.

Note that the proposed algorithm is executed once to satisfy delay requirement for the worst case in the current network topology, i.e. the maximum size of burst is sent from all the RUs. Then, the OLT continuously allocates the fixed bandwidth to each ONU using fixed wavelength channels based on the calculated solution. The upstream data received by the ONUs are forwarded to the OLT immediately on the basis of the predefined schedule without real-time computing. The proposed algorithm is executed again if the physical/virtual topology changes; an ONU is activated/deactivated depending on traffic demand in the area or an ONU is connected/disconnected to the PON system. The allocation problem is solved with a simple algorithm based on the descending sort by propagation delay. The detail of the proposed algorithm is introduced in the following sections.

B. Variables

The variables used in the formulation for the proposed algorithm are shown in Table III. The details of these variables are explained in the following explanation.

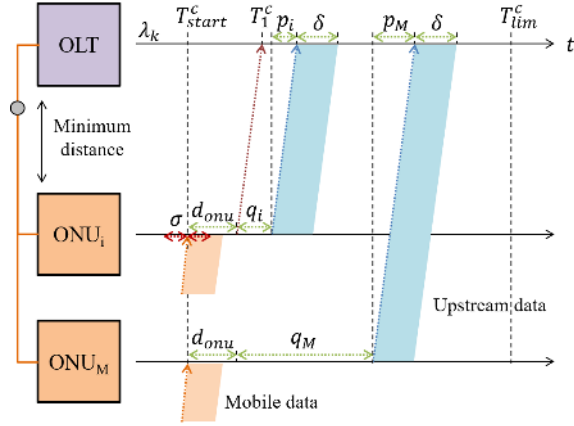


Fig. 7. Data transmission sequence.

C. Delay Formulation

The formulation for the delay components used in the proposed algorithm is explained here. Fig. 7 shows the fronthaul data transmission sequence in a wavelength channel using the defined variables. The ONUs time-synchronizedly receive the fronthaul data, which are time-synchronizedly sent from RUs. The propagation delay between RUs and ONUs is not different because each pair of an RU and an ONU is installed in the same antenna site. Let σ denote the synchronization time error value, which is determined by the synchronization category. It is given by absolute time error values from reference points, e.g. the master clock in PTP. The maximum burst size of the fronthaul stream is denoted as B .

It was assumed that the upstream bandwidth allocation is periodically executed. The upstream data reception timing at ONUs is determined by the TTI cycle in the C-RAN. This paper assumes that the leading point of the TTI cycle can be forecasted at the OLT using a traffic monitor in the same way as [40]. In other words, the start time of upstream traffic (shown as ‘‘U’’ in Fig. 5) is forecasted by the OLT. The traffic monitor captures the traffic and searches the switching period of traffic. Let c denote the identifier for upstream data transmission cycle in fronthaul, which is determined by the TTI cycle. The start time of c th cycle is denoted as T_{start}^c .

Let k denote the identifier for wavelength channels. The k th wavelength channel is also described as λ_k . K is the number of available wavelength channels determined by the system capacity. Let i denote the identifier for ONUs and the number of them is described as M . The processing delay in the ONUs is denoted as d_{onu} . Although the processing delay can fluctuate, d_{onu} represents the maximum value to consider the worst case delay. The queuing delay in i th ONU is formulated as q_i , which depends on the transmission start time of this ONU. The goal of the proposed algorithm is controlling q_i to satisfy the latency requirement. The propagation delay between i th ONU and the OLT is denoted as p_i . The maximum time period required for fronthaul data transmission is denoted as δ . This value depends on the maximum burst size and the link speed L , and is formulated as $\frac{B}{L}$.

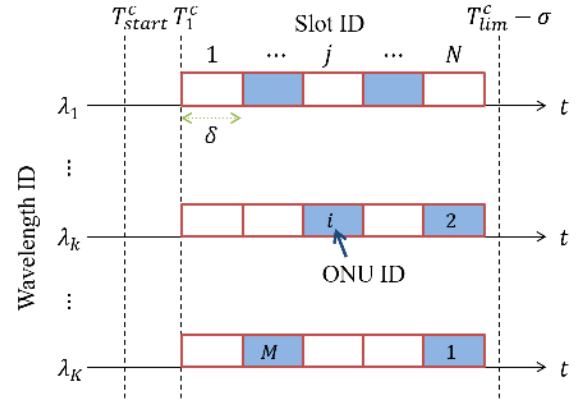


Fig. 8. Time slot.

The requirement for delay of i th ONU is formulated with the defined variables as:

$$d_i = d_{onu} + q_i + p_i + \delta \leq T_{lim}^c - T_{start}^c - 2\sigma, \quad (1)$$

where $(T_{lim}^c - T_{start}^c)$ denotes the allowable delay for fronthaul traffic in the PON system. From this value, 2σ is reduced to avoid the data transmission error or collision, because the data arrival at ONU can be late or early at most σ from T_{start}^c .

D. Time Slot

The proposed algorithm is based on the concept of time slot, which is depicted in Fig. 8. A time slot is allocated to an ONU, i.e. a fronthaul stream. A certain number of time slots are assigned to each wavelength channel at the OLT. The data sent from an ONU is received by the OLT using the allocated time slot. The length of a time slot is denoted as δ . δ is determined so that the maximum data burst of fronthaul can be safely transmitted. That is, the proposed algorithm allocates wavelength and bandwidth assuming the worst case to avoid data loss. It employs a safety allocation scheme to ensure low-latency and high reliability.

Let T_j^c denote the beginning of j th time slot of c th cycle ($j \geq 1$). It is formulated as:

$$T_j^c = T_{start}^c + \sigma + d_{onu} + p_{min} + (j - 1)\delta, \quad (2)$$

where p_{min} denotes the minimum propagation delay in the PON system as shown in Fig. 7. Let N denote the number of time slots. It is determined as:

$$N = \left\lfloor \frac{T_{lim}^c - \sigma - T_1^c}{\delta} \right\rfloor. \quad (3)$$

In (2), p_{min} can be set as the actual minimum value corresponding to the nearest ONU or the predefined value. In the former case, the actual minimum value must be measured and used. The number of time slots is optimized and the bandwidth utilization is maximized. In the latter case, although there is no need for measuring the actual latency. If an appropriate value is predefined, it is always valid regardless of the physical topology.

ONUs send upstream data using the assigned wavelength channel so that the data are received by the OLT at the

allocated time slot. Note that the minimum data arrival time is determined for each ONU considering the processing and propagation delay. An ONU cannot be assigned to the time slot that starts before the minimum data arrival time of the ONU. Let τ_i denote the minimum time slot for i th ONU. τ_i is formulated as:

$$\tau_i = \text{Min } j \quad \text{s.t. } T_j^c \geq T_{start}^c + \sigma + d_{onu} + p_i. \quad (4)$$

When ONUs are assigned to any of the defined time slots, the delay requirement formulated in (1) is satisfied for all of them. This is because the end of N th time slot ($T_N^c + \delta$) is less than the threshold considering the error value, which is given as $T_{lim}^c - \sigma$. The time slot allocation algorithm is described below.

E. Allocation Algorithm

The proposed allocation algorithm is introduced in the following. First, we explain the problem definition in III-E1 to clarify the goal of the allocation. Second, the allocation algorithm is described in III-E2 to solve the defined problem and obtain the optimum solution. Next, the mathematical proof of the optimality with the proposed algorithm is described in III-E3. Then, it is explained in III-E4 that the proposed algorithm is a polynomial time one and the computational complexity is $\mathcal{O}(M)$. Finally, the practical applicability of the proposed algorithm is discussed in III-E5.

1) *Problem Definition*: The goal of the proposed algorithm is to minimize the number of active wavelength channels to improve the energy-efficiency and deployment cost, which is formulated with the defined variables as

$$\text{Min } \sum_k w_k. \quad (5)$$

With this objective, more fronthaul streams can be accommodated with small number of wavelength channels, and consequently the energy-efficiency and deployment cost are improved.

We define the following binary variables for representing the allocation states of each ONU. The allocation state of i th ONU for j th time slot is represented by x_{ij} ; if i th ONU is allocated to j th slot, $x_{ij} = 1$; otherwise, $x_{ij} = 0$. The allocation state of i th ONU for k th wavelength is represented by y_{ik} ; if i th ONU is allocated to k th channel, $y_{ik} = 1$; otherwise, $y_{ik} = 0$. The activation state of k th channel is represented by w_k ; if k th wavelength channel is active, $w_k = 1$; otherwise, $w_k = 0$.

With defined binary variables, the constraints for allocating the wavelength channels and time slots to the ONUs are formulated as the following. First, an ONU is assigned to one of the wavelength channels, which is expressed as

$$\sum_k y_{ik} = 1 \quad \forall i. \quad (6)$$

Also, an ONU is assigned to one of the time slots as

$$\sum_j x_{ij} = 1 \quad \forall i. \quad (7)$$

To avoid the collision of optical signals, multiple ONUs cannot be allocated to the same time slot, i.e. only one ONU can be allocated to a time slot, which is formulated as

$$\sum_i x_{ij} y_{ik} \leq 1 \quad \forall j, k. \quad (8)$$

In addition, a major constraint for the allocation is the available time slots for each ONU defined in III-D. This constraint is formulated as

$$\sum_{j=1}^{\tau_i-1} x_{ij} = 0 \quad \forall i, \quad (9)$$

which represents that there is a minimum time slot available for each ONU due to the minimum data arrival time. Finally, a wavelength channel is activated if one or more ONUs are allocated for this channel as

$$w_k \geq y_{ik} \quad \forall i, k. \quad (10)$$

2) *Algorithm*: The goal of the proposed algorithm is to obtain the optimum solution that can achieve (5) satisfying the constraints formulated in (6)–(10).

The proposed algorithm is based on the fact that if the allocated time slots of ONUs are determined in the descending order of propagation delay for the ONUs, the most uncrowded time slot is always available. With the proposed algorithm, the variables are fixed to satisfy the constraints (6) – (10). The computed solution minimizes the objective function (5), which is mathematically proven in III-E3. The detail of the proposed algorithm is introduced in the following.

The ONU identifier i is re-assigned in the descending order by the propagation delay p_i . In addition, we define $X_i = \{x_{i1}, x_{i2}, \dots\}$ and $Y_i = \{y_{i1}, y_{i2}, \dots\}$. The overall sequence of the proposed algorithm is described in Algorithm 1.

The proposed algorithm determines the allocated wavelength and time slots for ONUs in the sequence of i ($1 \leq i \leq M$). First, X_i and Y_i are initialized (line 1 – 3). Then, the allocation procedure is executed for each ONU (line 4 – 18). The value of h_i is calculated (line 5 – 8), where h_i denotes the minimum number of ONUs allocated to a time slot among the time slots to which i th ONU can be allocated. The allocatable time slots for this ONU is calculated with (9) based on (4). The proposed algorithm finds the latest time slot to which i th ONU can be allocated and the number of ONUs already allocated is equal to h_i (line 9 – 12). The found time slot is defined as α_i . Then, it finds the wavelength channel with minimum k of which no ONU is allocated to α_i th time slot, which is formulated in (8) (line 13 – 16). The found wavelength channel defined as β_i . Finally, i th ONU is allocated to α_i th time slot and β_i th wavelength channel satisfying (6) and (7) (line 17 – 18). After the allocation of all ONUs, the state of each wavelength channel w_k is then automatically decided with (10) to minimize the objective $\sum_k w_k$ (line 19 – 23). Because $\tau_i \leq \tau_{i-1}$ is satisfied, the range of available time slots for i th ONU is always larger than that of $i-1$ th ONU. Thus, the most uncrowded time slot is always available for all i and consequently the active wavelength channels are minimized.

Algorithm 1 Allocation Algorithm

```

1: for  $i = 1$  to  $M$  do
2:    $X_i = \mathcal{O}$ 
3:    $Y_i = \mathcal{O}$ 
4: for  $i = 1$  to  $M$  do
5:    $h_i = M$ 
6:   for  $j = \tau_i$  to  $N$  do
7:     if  $\sum_i x_{ij} < h_i$  then
8:        $h_i = \sum_i x_{ij}$ 
9:   for  $j = N$  to  $\tau_i$  do
10:    if  $\sum_i x_{ij} = h_i$  then
11:       $\alpha_i = j$ 
12:      Break
13:   for  $k = 1$  to  $K$  do
14:    if  $\sum_i x_{i\alpha_i} y_{ik} = 0$  then
15:       $\beta_i = k$ 
16:      Break
17:    $x_{i\alpha_i} = 1$ 
18:    $y_{i\beta_i} = 1$ 
19: for  $k = 1$  to  $K$  do
20:   if  $y_{ik} = 0 \forall i$  then
21:      $w_k = 0$ 
22:   else
23:      $w_k = 1$ 

```

If the traffic does not allow a feasible solution of the problem, i.e. the required number of wavelength channels exceeds the system capacity, the network operators must consider changing the physical topology such as reconnecting some ONUs to other PON systems. This is because the number of accommodated fronthaul streams exceeds the capacity of the employed PON system.

3) *Mathematical Proof*: Here we present the mathematical proof that the number of active channels is minimized with the proposed algorithm. That is, it is proven that the computed solution minimizes the objective function (5). Since the variables are fixed in the proposed algorithm to meet the constraints (6) – (10), this section also mathematically proves that the proposed algorithm can obtain the optimum solution of the formulated optimization problem. The proof is based on mathematical induction.

(i) First, $x_{ij} = 0$ and $y_{ik} = 0$ are set for all i, j , and k in the initialization process. When $i = 1$,

$$h_1 = \text{Min} \sum_i x_{ij} = 0. \quad (11)$$

With $h_1 = 0$, α_1 is computed as

$$\begin{aligned} \alpha_1 &= \text{Max } j \text{ s.t. } \tau_1 \leq j \leq N \cap \sum_i x_{ij} = h_1 = 0 \\ &= N. \end{aligned} \quad (12)$$

With $\alpha_1 = N$, β_1 is calculated as

$$\begin{aligned} \beta_1 &= \text{Min } k \text{ s.t. } \sum_i x_{iN} y_{ik} = 0 \\ &= 1. \end{aligned} \quad (13)$$

With α_1 and β_1 , $x_{1N} = 1$ and $y_{11} = 1$ are fixed. Consequently, $w_k = 1$ is satisfied only if $k = 1$. The number of active channel is calculated as

$$\sum_k w_k = 1, \quad (14)$$

which is the minimum value. It is confirmed that the objective function (5) is minimized.

(ii) Assume that when $i = n$, the number of active channel is minimized, i.e. the objective function (5) is minimized. Let \mathcal{J}_n^h denote the set of j that satisfies $\tau_n \leq j \leq N \cap \sum_i x_{ij} = h_n$ at the allocation n th ONU (Line 6 in Algorithm 1 with $i = n$). $j \in \mathcal{J}_n^h$ is denoted as j_1^h, j_2^h, \dots ($j_1^h > j_2^h > \dots$). With these variables, $\alpha_n = j_1^h$ and $x_{n\alpha_n} = 1$ are fixed for $i = n$. After the allocation of n th ONU,

$$\sum_i x_{i\alpha_n} = h_n + 1. \quad (15)$$

When $i = n + 1$, $p_{n+1} \leq p_n$ is satisfied because i is sorted in the descending order using p_i . From (4), $\tau_{n+1} \leq \tau_n$ is satisfied if $p_{n+1} \leq p_n$.

Lemma 1: Given $\tau_{n+1} \leq \tau_n$, there are the following three cases for h_{n+1} .

- 1) $h_{n+1} = 0$
- 2) $h_{n+1} = h_n$
- 3) $h_{n+1} = h_n + 1$

Proof: If $\tau_{n+1} < \tau_n$, $\tau_{n+1} < \tau_i$ is satisfied for all i ($1 \leq i \leq n$). Thus,

$$h_{n+1} = \sum_i x_{i\tau_{n+1}} = 0 \quad (16)$$

is fixed using $x_{i\tau_{n+1}} = 0 \forall i$, which is the case 1).

If $\tau_{n+1} = \tau_n$, there are two cases based on $|\mathcal{J}_n^h|$. When $|\mathcal{J}_n^h| > 1$,

$$\sum_i x_{ij_2^h} = h_n \quad (17)$$

is satisfied, and thus $h_{n+1} = h_n$, which is the case 2). When $|\mathcal{J}_n^h| = 1$,

$$\begin{aligned} h_{n+1} &= \text{Min} \sum_i x_{ij} \text{ s.t. } \tau_{n+1} \leq j \leq N \\ &= h_n + 1, \end{aligned} \quad (18)$$

because of (15), which is the case 3). ■

The minimality of the active channels is proven for each case of 1) – 3) in the following.

1) $h_{n+1} = 0$: $\alpha_{n+1} = \tau_{n+1}$ is fixed from the definition. Then, $\beta_{n+1} = 1$ is fixed because $x_{i\alpha_{n+1}} y_{i1} = 0 \forall i$. With α_{n+1} and β_{n+1} , $x_{n+1, \tau_{n+1}} = 1$ and $y_{n+1, 1} = 1$ are fixed. Consequently, w_k is unchanged for all k ; the number of active channels stays minimal.

2) $h_{n+1} = h_n$: As stated before, j_2^h is the largest j that satisfies $\tau_{n+1} \leq j \leq N \cap \sum_i x_{ij} = h_n$. That is, $\alpha_{n+1} = j_2^h$ is fixed. $h_n = \gamma$ represents that the number of i that satisfies $x_{ij_2^h} = 1$ is γ . Also, the number of i that satisfies $\alpha_i = j_2^h$ is γ . Let us define

$$\mathcal{I} = \{\iota_1, \iota_2, \dots, \iota_\gamma\} \quad (\iota_1 < \iota_2 < \dots < \iota_\gamma) \quad (19)$$

as the set of i that satisfies the above conditions. From the definition of β_i ,

$$y_{i1} = 1, \quad y_{i2} = 1, \dots, y_{i\gamma} = 1 \quad (20)$$

is satisfied. Thus,

$$\beta_{n+1} = \gamma + 1 = h_n + 1. \quad (21)$$

With α_{n+1} and β_{n+1} , $x_{n+1,j_2^k} = 1$ and $y_{n+1,h_n+1} = 1$ are fixed. The values of w_k are unchanged because $w_{h_n+1} = 1$ is already satisfied from (15). Therefore, the number of active channels does not increase and stays minimum.

3) $h_{n+1} = h_n + 1$: Since $\tau_{n+1} < \tau_i$ is satisfied for all i ($1 \leq i \leq n$), $h_{n+1} = h_n + 1$ means that

$$h_{n+1} = \sum_i x_{ij} \quad \forall j \text{ s.t. } \tau_{n+1} \leq j \leq N. \quad (22)$$

Thus, α_{n+1} is computed as

$$\begin{aligned} \alpha_{n+1} &= \text{Max } j \quad \text{s.t. } \tau_{n+1} \leq j \leq N \cap \sum_i x_{ij} = h_{n+1} \\ &= N. \end{aligned} \quad (23)$$

With $\alpha_{n+1} = N$, β_{n+1} is calculated as

$$\begin{aligned} \beta_{n+1} &= \text{Min } k \quad \text{s.t. } \sum_i x_{iN} y_{ik} = 0 \\ &= h_{n+1} + 1. \end{aligned} \quad (24)$$

With α_{n+1} and β_{n+1} , $x_{1N} = 1$ and $y_{1,h_n+1+1} = 1$ are fixed. As a consequence, w_{h_n+1+1} becomes 1. The number of active channel is calculated as

$$\sum_k w_k = h_{n+1} + 1, \quad (25)$$

which is the minimum value. It is confirmed that the objective function (5) is minimized in all the cases of 1) – 3).

From the above, it was mathematically proven with mathematical induction that the number of active channels is minimized with the proposed algorithm. Therefore, the proposed algorithm can obtain the optimum solution of the formulated optimization problem, because the computed solution minimizes the objective function (5) and satisfies the constraints (6) – (10).

4) *Computational Complexity*: The computational complexity of the proposed algorithm is simply calculated as $\mathcal{O}((2N + K)M)$ from Algorithm 1. Here, note that the number of time slots N is a constant variable determined by the latency requirements and the burst size of fronthaul. For example, when we assume a simple condition where $T_{lim}^c = 250 \mu\text{s}$, $\sigma = 0$, $T_1^c = 0$, $B = 4 \times 10^5$ bit, and $L = 10$ Gb/s, $N = 6$ is obtained with (3). Also, the number of wavelength channels K is also a constant variable which is determined by the system capacity. When N and K in $\mathcal{O}((2N + K)M)$ are treated as constant variables, the computational complexity of the proposed algorithm can be described as $\mathcal{O}(M)$. Therefore, the proposed algorithm is a polynomial time one of the number of ONUs.

5) *Practical Applicability*: Here we discuss the practical applicability of the proposed algorithm. With the proposed scheme, the computed optimum solution is continuously applied until the physical/virtual topology of PON changes. The proposed algorithm is executed when an ONU is activated/deactivated depending on traffic demand in the area or an ONU is connected/disconnected to the PON system. Because of this feature, the computational complexity is not a significant issue for the proposed scheme. Until the re-allocation, time slots are continuously allocated in the same order with the same wavelength channels for each ONU, and thus tuning operations are infrequent. This is because the proposed algorithm allocates wavelength and bandwidth so that all data can always be forwarded satisfying the latency requirement in the current topology; even if all RUs simultaneously send upstream data of the maximum burst size, the end-to-end delay from RU to DU for each fronthaul stream does not exceed the delay threshold.

Since tuning operations are infrequent, the proposed algorithm basically assumes Class 3 tuning time class shown in Table II. The advantage of Class 3 devices is that they are inexpensive compared with Class 1 and 2 devices. With Class 3 devices, the tuning time is far larger than the length of an allocation cycle; an ONU that changes the wavelength channel must stop data forwarding for several hundreds of allocation cycles. If the tuning time is 50 ms and the length of an allocation cycle is 500 μs , the tuning process continues for 100 cycles. Because of this difference in the time-scale, the transition period where an ONU is in the tuning process is not considered and modeled in the proposed algorithm. That is, the proposed scheme only needs to compute the state of an allocation cycle after the tuning, not during the tuning process. The ONU in the transition period does not have an effect on the allocation result. After the tuning finishes, the ONU starts upstream data transmission based on the computed schedule in the next allocation cycle. In other words, the drawback of changing the wavelength channel is the stop of data forwarding during the tuning time. Since the proposed scheme continuously allocates bandwidth in fixed channels with the computed optimum solution, it can minimize such stop of data forwarding.

Therefore, the proposed algorithm is highly applicable for practical systems because of two major reasons; 1) the proposed algorithm is a polynomial time one and the computational complexity is $\mathcal{O}(M)$ as described in III-E4. 2) the proposed algorithm minimizes the stop of data forwarding due to a wavelength tuning process by continuous allocation of bandwidth in fixed channels with the computed solution.

IV. NUMERICAL RESULTS

The performance of the proposed wavelength and bandwidth allocation algorithm was evaluated with computer simulations.

A. Topology and Parameters

Fig. 9 shows the simulated topology used in the evaluation. The simulation was executed with the self-developed simulator written in C++. The OLT was connected to M ONUs using

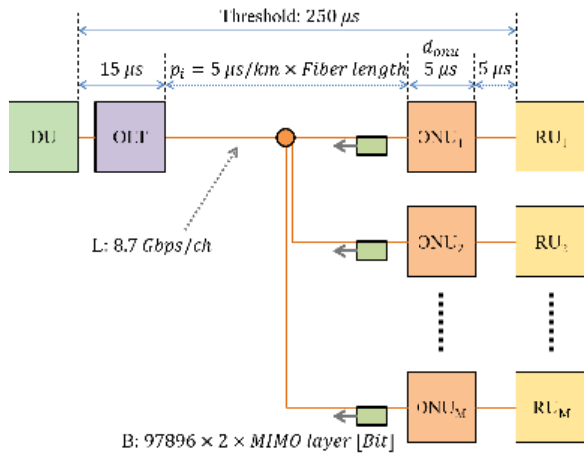


Fig. 9. Simulation condition.

optical fibers. The setting of M at each condition is described in the following sections. The delay threshold for mobile fronthaul traffic was set at $250 \mu\text{s}$ [5]. For the allowable delay in the PON system ($T_{lim}^c - T_{start}^c$) was assumed to be $230 \mu\text{s}$, where the delay of the RU-ONU and the OLT-DU was set to $5 \mu\text{s}$ and $15 \mu\text{s}$, respectively as shown in Fig. 9. These delay values were set considering propagation and packet processing delay, and do not affect the performance of the proposed algorithm. The propagation delay was $5 \mu\text{s}/\text{km}$. The upstream link bandwidth L was $8.7 \text{ Gbps}/\text{ch}$, which considers the overhead in the PON system. The distance between the OLT and each ONU was randomly determined. The burst size is set based on [41] considering the 5G parameters and the functional splitting option 6. That is, the burst size is determined by $S_{TB}N_{TB}N_{MIMO}$, where S_{TB} denotes transport block size, N_{TB} denotes the number of transport block per subframe, and N_{MIMO} is the number of MIMO layers. In this case, $S_{TB} = 97896$ bits and $N_{TB} = 2$. N_{MIMO} was set to 1, 2, and 4. Each RU synchronously sends the maximum burst every 1ms to simulate TDD. The ONUs send upstream data the predefined schedule calculated with and without the proposed technique. Since the delay requirement of mobile fronthaul is to finish forwarding data in the defined threshold, the worst case where all ONUs simultaneously send upstream data of the maximum burst size was considered in the simulation. That is, the latency changes with the change of the load were not evaluated because it is obvious that the latency requirements are satisfied at low load if they are satisfied in the worst case. The synchronization timing error was set as category C ($1.5\mu\text{s}$). The limitations for wavelength channels and the number of ONUs were not considered in the simulation. The parameters used in the simulation are summarized in Table IV.

B. Verification Items

1) *Delay Distribution*: First, it was confirmed that the wavelength channels and upstream bandwidth can be allocated to each ONU with the proposed algorithm to satisfy the latency requirements; the worst case delay does not exceed the delay threshold. The allocation was executed with the proposed algorithm in 100 times iterations with different

TABLE IV
SIMULATION PARAMETERS

Parameter	Value
Delay threshold	$250 \mu\text{s}$
Propagation delay	$5 \mu\text{s}/\text{km}$
B	$97896 \times 2 \times N_{MIMO}$
L	8.7 Gb/s
N_{MIMO}	1, 2, 4
σ	$1.5 \mu\text{s}$

ONU distributions. For each iteration, the distance between the OLT and each ONU was randomly determined with uniform distribution ranging from 0 to 20 km. The number of ONUs M was fixed at 100. After the allocation, the end-to-end delay from RU to DU for each fronthaul stream was measured.

2) *Active Wavelength Channels*: Second, the number of active wavelength channels was counted with different number of ONUs up to 50. 50 cases of different random distributions were simulated for each number of ONUs. The conditions for random variables were the same as section IV-B1. The performance of the proposed algorithm was compared with that of a conventional algorithm used by network operators. In the conventional algorithm, the wavelength channels and fixed bandwidth are allocated to ONUs assuming the fixed delay including processing and propagation delay ($5\mu\text{s} \times 20 \text{ km}$), without taking the difference of propagation distance into account.

3) *Synchronization Timing Error*: Third, we evaluated the effect of considering synchronization timing error. Without this consideration, two types of data transmission failure can occur;

- 1) If mobile data arrives late for the ONU to which the 1st time slot is allocated, the time slot can start before the data arrival finishes.
- 2) If mobile data arrives early for the ONU to which the N th time slot is allocated, the latency requirement cannot be satisfied.

To evaluate these failures, the occurrence probability for each failure was calculated based on the following assumptions. An ONU with the minimum propagation delay p_{min} receives mobile data with random timing error, and one of the time slots is randomly assigned to this ONU. The random variables are uniformly distributed.

C. Result

1) *Delay Distribution*: Fig. 10 shows the distribution of measured end-to-end delay for each fronthaul stream in each condition. The points represent the average, and the error bars represent the minimum and maximum values. The delay values range from about $50 \mu\text{s}$ to $248 \mu\text{s}$ in each case. For all iterations, the worst case delay (maximum value) does not exceed the threshold of $250 \mu\text{s}$. This result indicates that the delay requirement for fronthaul transmission is satisfied for all streams in all iterations. It was confirmed from this result that the proposed algorithm can properly allocate the wavelength channels and bandwidth to each ONU satisfying the requirements.

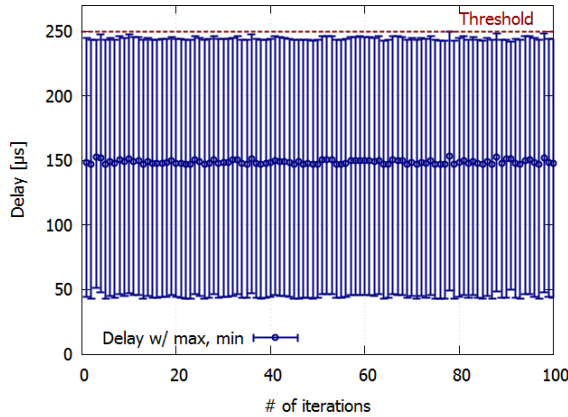


Fig. 10. Delay distribution.

2) *Active Wavelength Channels*: Figs. 11a–11c show the average number of active wavelength channels for different number of ONUs with $N_{MIMO} = 1, 2, \text{ and } 4$, respectively. It was shown that the number of active channels was reduced by 50% with the proposed algorithm irrespective of the number of MIMO layers, compared with the algorithm without the proposed technique. For example of an NG-PON2 [12] system, about 40 ONUs are connectable using four wavelength channels with the proposed algorithm, whereas less than 20 ONUs without it in Fig. 11a.

3) *Synchronization Timing Error*: There are two cases for timing error; a) the 1st time slot starts before the data arrival, and b) the end of the N th time slot exceeds the requirement T_{lim}^c .

First, we describe the case a), i.e. the failure for the 1st time slot. Without the consideration for the timing error, the start time of the 1st time slot is formulated as:

$$T_1^c = T_{start}^c + d_{onu} + p_{min}. \quad (26)$$

From (2) and (26), if $\sigma > 0$, i.e. the data arrival time is late from T_{start}^c , the time slot starts before the data arrival. The probability that the 1st time slot is allocated to this ONU is $\frac{1}{N}$. From (2), T_j^c including T_1^c increases if p_{min} increases. When T_1^c increases, N decreases from (3). Thus, the relationship between the failure probability and p_{min} is calculated as Fig. 12. The failure probability is independent from the synchronization category and increases with p_{min} . With the timing error consideration, the failure probability is always 0.

Second, the case b), i.e. failure for the N th time slot, is described. As shown in Fig. 8 and (2), the beginning of the 1st time slot is determined by p_{min} . The number of time slots N and the end of the N th time slot is also decided by p_{min} . Let t_{diff} denote the difference between the end of N th time slot and T_{lim}^c . Whether the transmission failure can occur by the timing error or not is determined by t_{diff} . That is, the transmission failure can occur if t_{diff} is small compared to σ . Without the timing error consideration, t_{diff} is formulated as:

$$t_{diff} = T_{lim}^c - (T_N^c + \delta). \quad (27)$$

Using (27), the range of t_{diff} is computed as shown in Fig. 13 for the category C. As a result, the relationship between the failure probability and p_{min} is calculated as Fig. 14. There are peaks at $p_{min} = 15, 50, 85$ without error consideration in Fig. 14, because t_{diff} can be less than 0 at $p_{min} = 15, 50, 85$ as shown in Fig. 13. For example, in the case of $p_{min} = 15$, there are 24 time slots ($N = 24$) and $T_{lim}^c - T_N^c = 1.2\mu s$. When p_{min} becomes 20, N decreases to 23 and $T_{lim}^c - T_N^c$ increases to $4.9\mu s$. Thus, the case b) error can occur certain conditions without error consideration. However, in the same way as the 1st time slot, the failure probability is always 0 with the timing error consideration.

D. Discussion

The reason why the number of active wavelength channels can be reduced by 50% with the proposed algorithm is that the proposed algorithm allocates bandwidth considering the difference in data arrival time caused by the different propagation delay between the OLT and ONUs. In this case, the length of a time slot calculated with the link speed and burst size is $22.5 \times N_{MIMO}\mu s$. This value is equivalent to the propagation delay for $4.5 \times N_{MIMO}$ km. The number of available slots is decremented as the transmission distance increases by $4.5 \times N_{MIMO}$ km. In other words, if two ONUs the distance difference of which is $4.5 \times N_{MIMO}$ km send data at the same time, the two bursts arrive at the OLT in the completely different timing. Since the proposed algorithm utilizes the difference of propagation delay for minimizing active channels, the effect of the proposed algorithm is easily maximized if there are more near ONUs with a large number of available time slots. The condition where both average and standard deviation of distance are large represents that both near and distant ONUs are connected. In this case, the distant ONUs are first assigned to the later time slots, and then near ONUs are assigned to earlier time slots that are unavailable for distant ONUs. Consequently, the bandwidth for each channel is efficiently utilized with the proposed algorithm.

The proposed scheme does not need any special or expensive optical device. This is because it does not require high-speed wavelength tuning. Generally, expensive optical devices are required for high-speed wavelength tuning. For example, three tuning time classes are defined in NG-PON2 standard [12]. The requirements for tuning time are $< 10\mu s$ for Class 1, $10\mu s - 25 ms$ for Class 2, and $25 ms - 1 s$ for Class 3. To satisfy the requirement for Class 1, expensive devices must be employed. From this perspective, Class 3 is sufficient for executing the proposed wavelength allocation, because it only allocates wavelength channels if an ONU is newly connected to the system. Since the proposed allocation algorithm is very simple, the implementation and execution of it is also easy. It only needs the propagation delay between the OLT and each ONU, which is accurately measured in PON systems as a general function.

In the computer simulation, we considered a specific 5G class corresponding to the transmission parameters including the delay threshold and the burst size. Namely, we considered the functional splitting option 6 (MAC-PHY split) defined in 3GPP TR36.213 [41]. The reason why we employed the

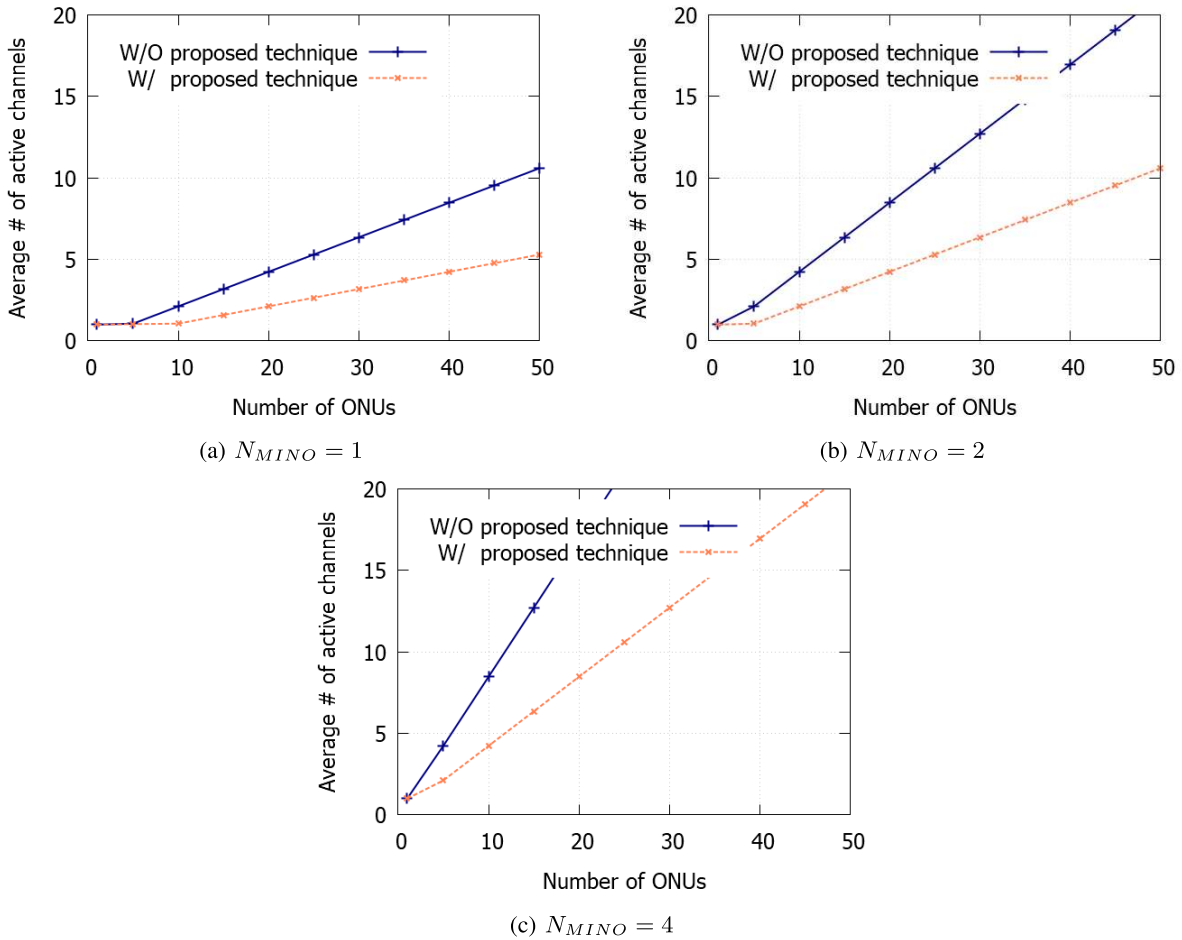


Fig. 11. Active wavelength channels.

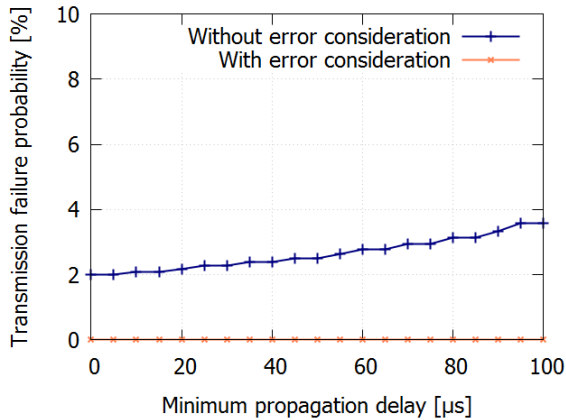


Fig. 12. Failure probability for 1st time slot.

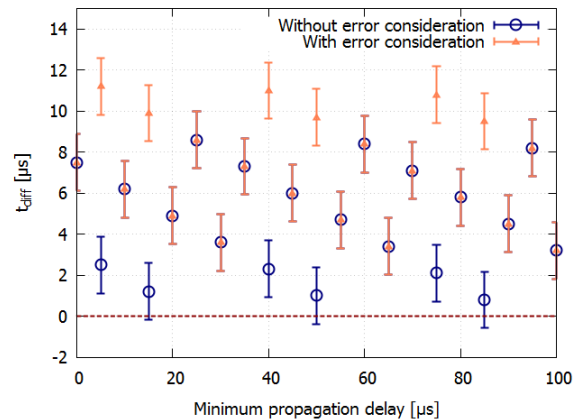


Fig. 13. Range of t_{diff} .

option 6 is that the transmission bit rate in the option 7-2 (eCPRI) is rather large for the currently general PON such as NG-PON2 where four 10 Gb/s wavelength channels are available [42], [43]. The higher-speed PON can be employed for accommodating eCPRI. As regards eCPRI, the distribution burst traffic is determined by either TTI or orthogonal frequency division multiplexed (OFDM) symbol intervals [43]. If the fronthaul traffic is distributed with OFDM symbol

intervals, the proposed algorithm cannot be employed because it is difficult to forecast the arrival time of upstream data with a traffic monitor. On the contrary, if the fronthaul traffic is distributed with TTI, the proposed scheme can be employed in the same way as the option 6. In this case, the proposed algorithm can be executed independent of the link speed and the number of wavelength channels. Thus, it is effective and can be employed for the option 6 mobile fronthaul with

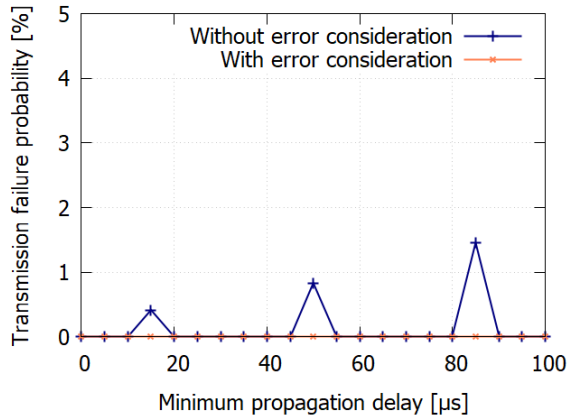


Fig. 14. Failure probability for N th time slot.

currently available 40 Gb/s PON systems, and other options such as eCPRI with higher-speed PON.

V. CONCLUSION

The traffic distribution of mobile fronthaul is expected to become highly bursty in TWDM-PON. This is because of the variable data rate caused by the change in functional split from CPRI and the synchronization of data transmission between neighboring RUs with the TDD systems. However, there has been no existing wavelength and upstream bandwidth allocation scheme that is designed to efficiently accommodate multiple ONUs with TWDM-PON satisfying the strict delay requirement for fronthaul. Therefore, this paper proposed a novel wavelength and bandwidth allocation algorithm for TWDM-PON with mobile fronthaul traffic with the consideration for TDD synchronization timing error. The goal of the proposed scheme is to minimize the number of active wavelength channels. To this end, it considers the maximum burst size of fronthaul, data reception timing, and difference in propagation delay between the OLT and ONUs. The allocation problem is formulated with these variables and is solved with the simple algorithm, whose computational complexity is $\mathcal{O}(M)$. The performance of the proposed algorithm was confirmed via computer simulations. It was shown that the number of active wavelength channels was reduced by 50% with the proposed algorithm compared with the algorithm without the proposed technique. This result was irrespective of the number of MIMO layers. Therefore, RUs in the C-RAN architecture can be efficiently accommodated in TWDM-PON with the proposed algorithm.

REFERENCES

- [1] A. Pizzinat, P. Chanclou, T. Diallo, and F. Saliou, "Things you should know about fronthaul," *J. Lightw. Technol.*, vol. 33, no. 5, pp. 1077–1083, Mar. 1, 2015.
- [2] Y. Kishiyama, A. Benjebbour, T. Nakamura, and H. Ishii, "Future steps of LTE-A: Evolution toward integration of local area and wide area systems," *IEEE Wireless Commun.*, vol. 20, no. 1, pp. 12–18, Feb. 2013.
- [3] P. Chanclou, L. A. Neto, K. Grzybowski, Z. Tayq, F. Saliou, and N. Genay, "Mobile fronthaul architecture and technologies: A RAN equipment assessment [invited]," *J. Opt. Commun. Netw.*, vol. 10, no. 1, pp. A1–A7, Jan. 2018.
- [4] *Common Public Radio Interface (CPRI); eCPRI Interface Specification V1.0*, Aug. 2017.
- [5] *Study on New Radio Access Technology: Radio Access Architecture and Interfaces*, document 3GPP TR 38.801, Mar. 2016.
- [6] "Next generation mobile networks," NGMN Alliance, 5G White Paper, Frankfurt, Germany, White Paper, Feb. 2015.
- [7] Y. Nakayama, K. Maruta, T. Shimada, T. Yoshida, J. Terada, and A. Otaka, "Utilization comparison of small-cell accommodation with PON-based mobile fronthaul," *J. Opt. Commun. Netw.*, vol. 8, no. 12, pp. 919–927, Dec. 2016.
- [8] P. Chanclou *et al.*, "Optical fiber solution for mobile fronthaul to achieve cloud radio access network," in *Proc. Future Netw. Mobile Summit (FutureNetworkSummit)*, Jul. 2013, pp. 1–11.
- [9] *Scenarios and Requirements for Small Cell Enhancements for E-Utra and E-Utran*, document TR 36.932, v12.1.0, 3GPP, Mar. 2013.
- [10] *10G-EPON*, IEEE Standard 802.3av, Oct. 2009.
- [11] *10 Gigabit-Capable Passive Optical Network (XG-PON)*, document ITU-T G.987 Series Recommendations, Jun. 2012.
- [12] *40-Gigabit-Capable Passive Optical Networks 2 (NG-PON2)*, document ITU-T G.989 Series Recommendations, Oct. 2015.
- [13] D. Nessel, "NG-PON2 technology and standards," *J. Lightw. Technol.*, vol. 33, no. 5, pp. 1136–1143, Mar. 1, 2015.
- [14] Y. Luo *et al.*, "Time- and wavelength-division multiplexed passive optical network (TWDM-PON) for next-generation PON stage 2 (NG-PON2)," *J. Lightw. Technol.*, vol. 31, no. 4, pp. 587–593, Feb. 15, 2013.
- [15] S. Kuwano, J. Terada, and N. Yoshimoto, "Operator perspective on next-generation optical access for future radio access," in *Proc. IEEE Int. Conf. Commun.(ICC) Workshops*, Jun. 2014, pp. 376–381.
- [16] T. Tashiro *et al.*, "A novel DBA scheme for TDM-PON based mobile fronthaul," in *Proc. Opt. Fiber Commun. Conf.* Washington, DC, USA: OSA, Mar. 2014, pp. 1–3, Paper Tu3F-3.
- [17] Y. Nakayama *et al.*, "Efficient DWBA algorithm for TWDM-PON with mobile fronthaul in 5G networks," in *Proc. IEEE Global Telecommun. Conf. (GLOBECOM)*, Dec. 2017, pp. 1–6.
- [18] R. Vaez-Ghaemi, "The evolution of fronthaul networks," VIAVI Solutions, Milpitas, CA, USA, White Paper, 2017.
- [19] T. Yoshida, S. Kaneko, S. Kimura, and N. Yoshimoto, "An automatic load-balancing DWBA algorithm considering long-time tuning devices for λ -tunable WDM/TDM-PON," in *Proc. 39th Eur. Conf. Exhib. Opt. Commun. (ECOC)*. Edison, NJ, USA: IET, Sep. 2013, pp. 1–3.
- [20] S. B. Hussain, W. Hu, H. Xin, and A. M. Mikaeil, "Low-latency dynamic wavelength and bandwidth allocation algorithm for NG-EPON," *J. Opt. Commun. Netw.*, vol. 9, no. 12, pp. 1108–1115, Dec. 2017.
- [21] A. Buttaboni, M. D. Andrade, and M. Tornatore, "A multi-threaded dynamic bandwidth and wavelength allocation scheme with void filling for long reach WDM/TDM PONs," *J. Lightw. Technol.*, vol. 31, no. 8, pp. 1149–1157, Apr. 15, 2013.
- [22] S. B. Hussain, W. Hu, H. Xin, A. M. Mikaeil, and A. Sultan, "Flexible wavelength and dynamic bandwidth allocation for NG-EPONs," *J. Opt. Commun. Netw.*, vol. 10, no. 6, pp. 643–652, Jun. 2018.
- [23] K. Kanonakis and I. Tomkos, "Improving the efficiency of online upstream scheduling and wavelength assignment in hybrid WDM/TDMA EPON networks," *IEEE J. Sel. Areas Commun.*, vol. 28, no. 6, pp. 838–848, Aug. 2010.
- [24] M. P. I. Dias, D. P. Van, L. Valcarengi, and E. Wong, "Energy-efficient framework for time and wavelength division multiplexed passive optical networks," *J. Opt. Commun. Netw.*, vol. 7, no. 6, pp. 496–504, Jun. 2015.
- [25] M. I. Dias *et al.*, "Energy-efficient dynamic wavelength and bandwidth allocation algorithm for TWDM-PONs with tunable VCSEL ONUs," in *Proc. 19th Optoelectron. Commun. Conf. (OECC), 39th Austral. Conf. Opt. Fibre Technol. (ACOFT)*, Melbourne, VIC, Australia, Jul. 2014, pp. 1007–1009.
- [26] L. Wang *et al.*, "Dynamic bandwidth and wavelength allocation scheme for next-generation wavelength-agile EPON," *J. Opt. Commun. Netw.*, vol. 9, no. 3, pp. B33–B42, Mar. 2017.
- [27] R. Wang *et al.*, "Energy saving via dynamic wavelength sharing in TWDM-PON," *IEEE J. Sel. Areas Commun.*, vol. 32, no. 8, pp. 1566–1574, Aug. 2014.
- [28] J. Kani, J. Terada, K.-I. Suzuki, and A. Otaka, "Solutions for future mobile fronthaul and access-network convergence," *J. Lightw. Technol.*, vol. 35, no. 3, pp. 527–534, Feb. 1, 2017.
- [29] G. Kramer, B. Mukherjee, and G. Pesavento, "IPACT a dynamic protocol for an Ethernet PON (EPON)," *IEEE Commun. Mag.*, vol. 40, no. 2, pp. 74–80, Feb. 2002.

- [30] T. Kobayashi, H. Ou, D. Hisano, T. Shimada, J. Terada, and A. Otaka, "Bandwidth allocation scheme based on simple statistical traffic analysis for TDM-PON based mobile fronthaul," in *Proc. Opt. Fiber Commun. Conf.* Washington, DC, USA: OSA, 2016, pp. 1–3, Paper W3C-7.
- [31] S. Hatta, N. Tanaka, and T. Sakamoto, "Low latency dynamic bandwidth allocation method with high bandwidth efficiency for TDM-PON," *NTT Tech. Rev.*, vol. 15, no. 4, pp. 1–7, 2017.
- [32] S. Hatta, N. Tanaka, and T. Sakamoto, "Feasibility demonstration of low latency DBA method with high bandwidth-efficiency for TDM-PON," in *Proc. Opt. Fiber Commun. Conf.* Washington, DC, USA: OSA, Mar. 2017, pp. 1–3, Paper M3I-2.
- [33] X. Wang *et al.*, "Energy-efficient virtual base station formation in optical-access-enabled cloud-RAN," *IEEE J. Sel. Areas Commun.*, vol. 34, no. 5, pp. 1130–1139, May 2016.
- [34] D. Iida, S. Kuwano, J.-I. Kani, and J. Terada, "Dynamic TWDM-PON for mobile radio access networks," *Opt. Express*, vol. 21, no. 22, pp. 26209–26218, 2013.
- [35] L. P. Liang, W. Lu, M. Tornatore, and Z. Q. Zhu, "Game-assisted distributed decision making to build virtual TDM-PONs in C-RANs adaptively," *IEEE J. Opt. Commun. Netw.*, vol. 9, no. 7, pp. 546–554, Jul. 2017.
- [36] Y. Nakayama, D. Hisano, T. Kubo, Y. Fukada, J. Terada, and A. Otaka, "Low-latency routing scheme for a fronthaul bridged network," *J. Opt. Commun. Netw.*, vol. 10, no. 1, pp. 14–23, Jan. 2018.
- [37] Y. Nakayama and D. Hisano, "Rank-based low-latency scheduling for maximum fronthaul accommodation in bridged network," *IEEE Access*, vol. 6, pp. 78829–78838, 2018.
- [38] *40-Gigabit-Capable Passive Optical Networks 2 (NG-PON2): Physical Media Dependent (PMD) Layer Specification*, document ITU-T Recommendation G.989.2, 2019.
- [39] J. S. Wey *et al.*, "Physical layer aspects of NG-PON2 standards—Part 1: Optical link design [Invited]," *J. Opt. Commun. Netw.*, vol. 8, no. 1, pp. 33–42, Jan. 2016.
- [40] D. Hisano *et al.*, "TDM-PON for accommodating TDD-based fronthaul and secondary services," *J. Lightw. Technol.*, vol. 35, no. 14, pp. 2788–2796, Jul. 15, 2017.
- [41] *E-UTRA Physical Layer Procedures*, document 3GPP TR 36.213 Release 14.4.0, Sep. 2017.
- [42] D. Hisano, H. Uzawa, Y. Nakayama, H. Nakamura, J. Terada, and A. Otaka, "Predictive bandwidth allocation scheme with traffic pattern and fluctuation tracking for TDM-PON-based mobile fronthaul," *IEEE J. Sel. Areas Commun.*, vol. 36, no. 11, pp. 2508–2517, Nov. 2018.
- [43] D. Hisano *et al.*, "Clarification of accommodatable number of functional split base stations in TDM-PON fronthaul," *IEICE Commun. Express*, vol. 7, no. 5, pp. 160–166, 2018.



Yu Nakayama (M'10) received the B.Agr. degree in agriculture, the M.Env. degree in environmental studies, and the Ph.D. degree in information and communication engineering from The University of Tokyo, Tokyo, Japan, in 2006, 2008, and 2018, respectively.

From 2008 to 2018, he was with NTT Access Network Service Systems Laboratories. He is currently an Associate Professor with the Institute of Engineering, Tokyo University of Agriculture and Technology. He is also the President of neko 9 Laboratories, which is a nonprofit organization in Tokyo. His research interests include mobile computing, network architecture, the IoT, and ultralow latency. He is a member of IEICE and IPSJ.



Daisuke Hisano (M'18) received the B.E., M.E., and Ph.D. degrees in electrical, electronic and information engineering from Osaka University, Osaka, Japan, in 2012, 2014, and 2018, respectively.

In 2014, he joined NTT Access Network Service Systems Laboratories, Yokosuka, Japan. Since October 2018, he has been an Assistant Professor with Osaka University. His research interests include optical-wireless converged networks, optical communication, and all-optical signal processing. He is a member of the Institute of Electronics, Information, and Communication Engineers (IEICE) of Japan.